Ecohydrology and causes of peat degradation at the Vasi peatland, South Africa

S. Elshehawi[1,2], M. Gabriel[3], L. Pretorius[4], S. Bukhosini[5],
M. Butler[6], J. van der Plicht[2], P. Grundling[7,8] and A.P. Grootjans[1,9]

[1] Centre for Energy and Environmental Studies, University of Groningen, The Netherlands
[2] Centre for Isotope Research, University of Groningen, The Netherlands
[3] Humboldt-Universität zu Berlin, Germany
[4] University of Kwazulu-Natal, South Africa
[5] Isibusiso Esihle Science Discovery Centre, South Africa
[6] iThemba LABS, Environmental Isotope Laboratory, South Africa.
[7] Centre for Environmental Management, University of the Free State, South Africa
[8] Working for Wetlands, NRM, Department of Environmental Affairs, Pretoria, South Africa
[9] Institute of Water and Wetland Research, Radboud University Nijmegen, The Netherlands

_____

SUMMARY

The Vasi peatland complex is situated in the northeast of South Africa. It is an unprotected area surrounded by pine (*Pinus* sp.) and blue gum (*Eucalyptus* sp.) plantations. Little is known about the conditioning factors for the area's development and causes of degradation. In order to understand the ecohydrological system of this complex, water tables and ionic composition of surface water and groundwater, as well as natural isotopes of oxygen, hydrogen and carbon, were measured. Macrofossils and radiocarbon dating of the peat layer were used to describe the historical environmental conditions. We found that peat accumulation started during the Early Holocene and was initiated by terrestrialisation of inter-dune lakes. Our results also show that the Vasi peatland complex is primarily dependent on a perched water table due to the presence of iron-rich deposits close to the surface (i.e. KwaMbonambi Formation). The Vasi peatland basins appear to be hydrologically connected and some basins show indications of cascading through-flow systems, which means that the water flows from a higher basin to a lower one through the permeable parts of the sand dunes and peat layers. The stratigraphy indicates continuous peat accumulation, and thus that the water table was perennially high for thousands of years, despite evidence of the occasional natural occurrence of fires. We conclude that the most likely cause of the observed signs of degradation is land use change, i.e. the recent establishment of plantations, which affect the groundwater system.

KEY WORDS: ecohydrology, natural isotopes, peat fires, radiocarbon dating

_____

INTRODUCTION

Peatlands are quite abundant in the Northern Hemisphere, but relatively rare in the Southern Hemisphere and even more so in its sub-tropical regions, e.g. South Africa (Joosten & Clarke 2002). In South Africa, around 60 % of the peatlands are situated along the coastline of Maputaland in northern KwaZulu-Natal Province (Grundling *et al.* 1998, Grundling & Grobler 2005). Peatlands in Maputaland range from forested peat swamps in valleys that drain upland areas or link inter-dune drainage lines with coastal lakes (Grundling *et al.* 2000), to sedge-dominated fens in inter-dune depressions (Grundling & Grobler 2005). Most of these systems started accumulating peat during the Holocene (Thamm *et al.* 1996, Grundling *et al.* 1998) but some date back to the Late-Pleistocene (Grundling & Grobler 2005, P. Grundling *et al.* 2013, Baker *et al.* 2014).

Peatlands in Maputaland primarily depend on groundwater supply (e.g. A.T. Grundling *et al.* 2013, Kelbe *et al.* 2016). Groundwater supply to the peatlands creates anoxic soil conditions and prevents rapid mineralisation of the peat (Mitsch & Gosselink 2000). Disturbance of the natural hydrological processes poses a threat to peatlands, e.g. by groundwater abstraction, afforestation, and eutrophication of water flows through intensive agricultural use (Maltby & Barker 2009).

During the last decade, drops in groundwater tables have been observed in large parts of Maputaland from the Muzi swamp in Tembe Elephant Park (Grundling 2014) in the west to the Manguzi area in the east and Lake Sibaya in the south (Weitz & Demilie 2014). The Vasi peatland complex is located in eastern Maputaland and is surrounded by expanding pine (*Pinus* sp.) and blue gum (*Eucalyptus* sp.) plantations (Figure 1a).
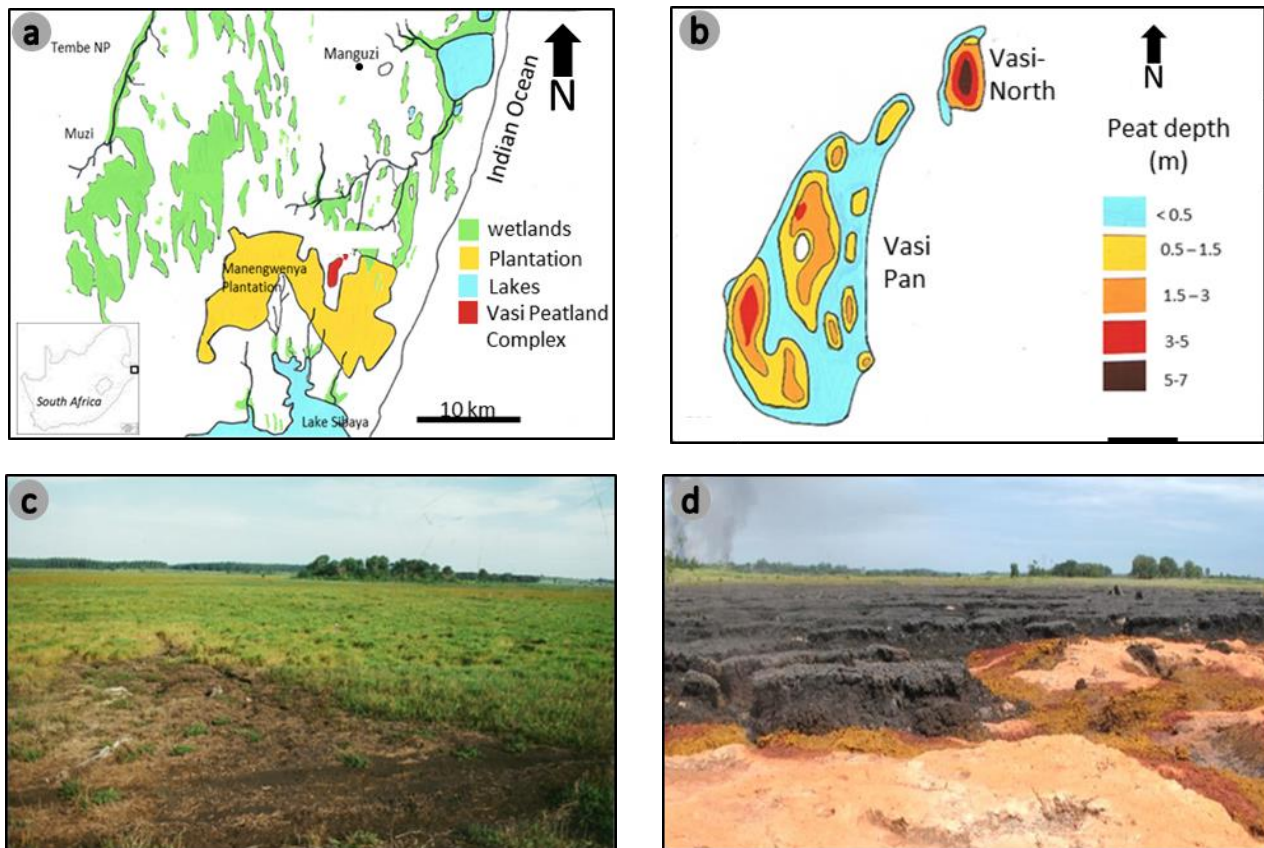
Figure 1. (a) Location of the study area: Vasi peatland complex (red), north of Lake Sibaya in KwaZulu-Natal, South Africa. The Vasi peatland complex is surrounded by the Manzengwenya plantations (yellow). (b) Peat depths in the Vasi peatland complex (source: Grundling & Blackmore 1998). (c) A photograph of one of the basins in Vasi Pan taken in 1998, with the (green) vegetation cover mostly intact. (d) A photograph of the same basin in March 2014. The vegetation cover has disappeared, 30–40cm of the peat has turned into ashes with widened fissures in between, and there are some indications of old spring sites which can be identified by the orange/brown colour of iron deposits.

According to local residents (S. Bukhosini, personal communication 2014) the water table in the Vasi peatlands has been dropping steadily for the last 20 years, and regular peat fires have been observed. Grundling & Blackmore (1998) reported severe burning of the peat in 1996 and suggested that fire risk might be reduced by removing relatively small sections of the tree plantations, which should have positive knock-on effects on water tables. However, they warned that this might not be sufficient in the long run as the period of their survey (1997–1998) had been characterised by high rainfall. More recently, peat fires have started again in the Vasi peatland complex, leading to an increased loss of peat and destruction of the sedge-dominated vegetation (Figures 1c and 1d).

Currently, the hydrological system of the Vasi peatland complex is not well understood. A.T. Grundling *et al.* (2013) and Kelbe *et al.* (2016) studied the relationships between water table depth and the spatial distribution and temporal functioning of wetlands in the northern Maputaland coastal plain. They concluded that the occurrence and development of wetlands was greatly influenced by topography at sub-regional level. Their studies further suggested that the permanent wetlands, which contain peat deposits up to 10 m thick, were maintained by a long-term regime of high and steady regional water table. The temporary wetlands were probably not connected to the regional water table, but may be important in providing water to wetlands at lower altitudes. Hence, the interaction between local and regional hydrological systems could be important for the maintenance of peatlands such as the Vasi peatland complex (A.T. Grundling *et al.* 2013, Kelbe *et al.* 2016).

Bate *et al.* (2016) also studied the effects of pine and blue gum plantations on hydrology, in the Mgobezeleni catchment area near the town of Mbazwana, using a hydrological model

(MODFLOW). They concluded that groundwater tables had dropped within and beyond the areas where plantations had been established. They calculated a significant drawdown of the water table due to both the dry climate cycle (which occurs every 20 years, see A.T. Grundling *et al.* 2013) and, more importantly, increased interception of precipitation and evapotranspiration by the vegetation canopies of the commercial plantations. The model revealed that, between 2004 and 2014, these combined effects had induced 7–9 metre deep cones of depression in water tables at the centres of the plantations.

In the present study we aim to gain a better understanding of the past and present hydrological functioning of the Vasi peatland complex. More specifically, we investigate whether the peatlands are fed by local hydrological systems or whether the groundwater supply is related to the larger regional hydrological system.

For insight into the origin of water flows, we used stable isotope ratios of hydrogen and oxygen (δ^2H and δ^{18}O) (Schot & van der Wal 1992, Gat 1996). If the Vasi peatlands are indeed influenced by regional groundwater with long residence times, we would expect to find groundwater with lower radiocarbon (^{14}C) values than in groundwater from local hydrological systems. In addition, if the present levels of severe peat degradation do not result from the expanding pine and blue gum plantations but rather from the recurring dry climate cycles, we would expect to find evidence of peat loss in the past as well as discontinuities in peat accumulation. Given the available time (less than three months) and the lack of long term water level data we used an ecohydrological system approach (Grootjans & van Diggelen 2009, Grootjans & Jansen 2012), in which we integrated macrofossil and stratigraphic research on past peat development with investigation of the present hydrological conditions. We described and dated peat profiles, measured water tables and ion composition, and analysed isotopic signatures and ^{14}C contents of groundwater and surface water in the Vasi complex and its wider surroundings.

The specific objectives are to: 1) investigate the possible interaction between local and regional groundwater systems in Maputaland and the origin of the groundwater supply to the Vasi peatland complex; 2) identify the hydrological flow directions and the possible hydrological linkages among the different basins in the complex; and 3) based on our own research and results of hydrological modelling from literature, try to verify whether the degradation of the Vasi peatlands is related to external land use management practices.

METHODS

Study site

The Vasi peatland complex (27° 11′ 12.31″ S, 32° 42′ 40.00″ E) is located in the northern part of the Maputaland coastal plain (MCP), 10 km inland from the Indian Ocean coastline at a height of 50–60 m above mean sea level (a.m.s.l., Grundling 2014). The Vasi peatland complex consists of several peatlands with varying peat depths (Figure 1b). Most of the peat deposits are situated in the area known as Vasi Pan. North of Vasi Pan lies a smaller peatland, Vasi-North, which has the thickest peat layer (5–7 metres). Both areas are surrounded by the Manzengwenya State Plantation, which was established in the 1960s (Thamm *et al.* 1996). Vasi Pan consists of three distinct basins separated by small sandy ridges running from south to north. Vasi-North is separated from Vasi Pan by a sandy ridge 300 m wide. The total area of Vasi Pan is about 210 ha, while Vasi-North covers only 12 ha (Grundling & Blackmore 1998). The Vasi peatlands have been used for livestock grazing by the inhabitants of the nearby village of Mvelabusha, and subsistence (vegetable) gardens have been maintained on the Vasi-North peatland in the past.

The average annual rainfall in Maputaland increases from 700 mm yr^{-1} in the Lebombo Mountains in the west to around 1100 mm yr^{-1} in the east; and the summer wet season lasts from November to March (P. Grundling *et al.* 2013). The catchment of the Vasi peatland complex receives up to 750–800 mm of rain per year and has a significant precipitation deficit, as the maximum potential evapotranspiration for this area is about 2200 mm yr^{-1} (Mucina & Rutherford 2006).

The primary aquifer in the Maputaland Coastal Plain consists of (from bottom to top) the Uloa, KwaMbonambi, Kosi Bay and Sibaya Formations. These strata overlie an aquiclude formation consisting of claystones and siltstones (Zululand Group), which is considered to be the base of the primary aquifer (Kelbe *et al.* 2016). The Uloa Formation consists of karst rocks with intercalated mudstones. However, in the eastern side of the plain it is overlain by an almost impervious layer (Port Durnford Formation) and Lignite, which separates it from the primary aquifer in this area (Botha *et al.* 2013, Kelbe *et al.* 2016). The Kosi Bay Formation is exposed to the surface at the Muzi swamp in the west (Figure 1a), while in the east it is overlain by the KwaMbonambi Formation close to the Vasi peatland complex (Figure 1a) (Porat & Botha 2008). The Kosi Bay Formation (which consists of sandy silts) and the

dune profile extensively cover the Maputaland Coastal Plain. Furthermore, the Kosi Bay Formation may contain interspaced clayey (lignite) and iron-rich soil layers (red sands), which can create perched local groundwater aquifers (Botha & Porat 2007). The KwaMbonambi Formation consists of reworked sand dunes which cover mostly the eastern parts of the Maputaland Coastal Plain, starting from the surroundings of the Vasi peatland complex. Important features of the study area are sandy parabolic ridges (Sibaya Formation) along the coast (Botha & Porat 2007). These ridges are aligned south–north (Botha *et al.* 2003), forming an upland area between the Pongola River valley (which drains northwards parallel to Lebombo Mountain) in the west, and the numerous coastal lakes in the east (Bruton 1980).

Description of stratigraphy

To investigate the stratigraphy of the Vasi-North substrates (at Core VN, see Figure 2a), a series of soil profile cores were taken using a Russian peat corer with a chamber length of 50 cm, with continuous cores in one hole, up to a total depth of about 8 m. The vertical extent of each horizon identified between the upper peat layer and the basal mineral layer was recorded. The peat profile from each core was described for colour, peat type and degree of decomposition (von Post Scale: H1–H10; von Post 1922), and for macrofossils following the reference scheme for South African peat deposits proposed by Gabriel *et al.* (2018). In this way, we described soil profiles along a transect (VNA1 to VNA4, hence a total of five cores at intervals of about 50 metres).

Radiocarbon dating of peat

For ^{14}C dating of the organic matter, soil samples were collected from two locations, Vasi-North (Core VN) and Vasi Pan (Core VP) (Figure 2a). The samples were taken from the cores as 1-cm sections directly above stratigraphic boundaries. The first core (VN) consisted of seven samples, while Core VP consisted of four samples. All samples were described in the field, then sealed into plastic bags and sent to the Centre for Isotope Research (CIO), University of Groningen (The Netherlands). They were treated using alkali-acid-alkali (AAA) to remove contaminants that might affect sample age and to isolate the datable organic fraction. This fraction was combusted to CO_2, then reduced to graphite (Aerts *et al.* 2001). The $^{14}C/^{12}C$ quotient of the graphite was measured by AMS (van der Plicht *et al.* 2000). Radiocarbon dates were calculated according to convention, i.e. using the oxalic acid reference, correction for isotopic fractionation based

on the δ^{13}C value of the sample, and the conventional half-life (Mook & van der Plicht 1999).

In general, conventional ^{14}C age is reported in years Before Present (BP). However, radiocarbon dates reported in BP need to be calibrated to historical (calendar) ages (calBP). In this case we used SHCal13, which is the most recent curve recommended for the calibration of Southern Hemisphere samples (Reimer *et al.* 2013). However, for modern samples influenced by the bomb peak (nuclear tests around 1950), other curves were constructed using the calibration for Regional Zones 1–2, i.e. valid for the southern hemisphere (Hua *et al*. 2013). We used OxCal software (Bronk Ramsey 2009) to calculate calibrations. This program yields calibrated age ranges that are not symmetrical or Gaussian because of fluctuations in the calibration curve. The 1σ (68.2 % probability) intervals were applied. Furthermore, to estimate layer-by-layer accumulation rates, we divided each layer's thickness by the difference in median calibrated ^{14}C age between the bottom and top boundaries.

Origin of groundwater flows

The schedule for studying the origin of groundwater flows was divided into two phases. The first phase, carried out in autumn 2015 (from February to July) focused on internal (small scale) observation of groundwater properties within the Vasi peatland complex catchment (Figure 2a). The aim of this first field campaign was to understand the flow origins (discharge and recharge areas) and directions within the Vasi peatland complex area. For the second phase, fieldwork was carried out in spring 2017 (October) and was aimed at the wider context of the Vasi peatland complex. We focused on different wetlands and rivers surrounding our study sites (Figure 2b) and analysed macro-ionic groundwater composition and isotopic contents of water (^{14}C, δ^{13}C, δ^2H and δ^{18}O) in order to estimate the origin and (relative) age of the groundwater.

Vasi peatland complex study (autumn 2015)

The first campaign, in the autumn of 2015, was carried out during a relatively wet period with falling water levels. The research focused on the Vasi-North basin and was supplemented with single points connecting to Vasi Pan (the southern part in Figure 2a). The low density of observation points within Vasi Pan is due to the frequent fires occurring there. Also, the water table in Vasi Pan was lower at the dune areas, where more costly deep drillings would be required. This campaign involved measuring water table depth (in perforated dipwells) and hydraulic head (in piezometers with filters only at the
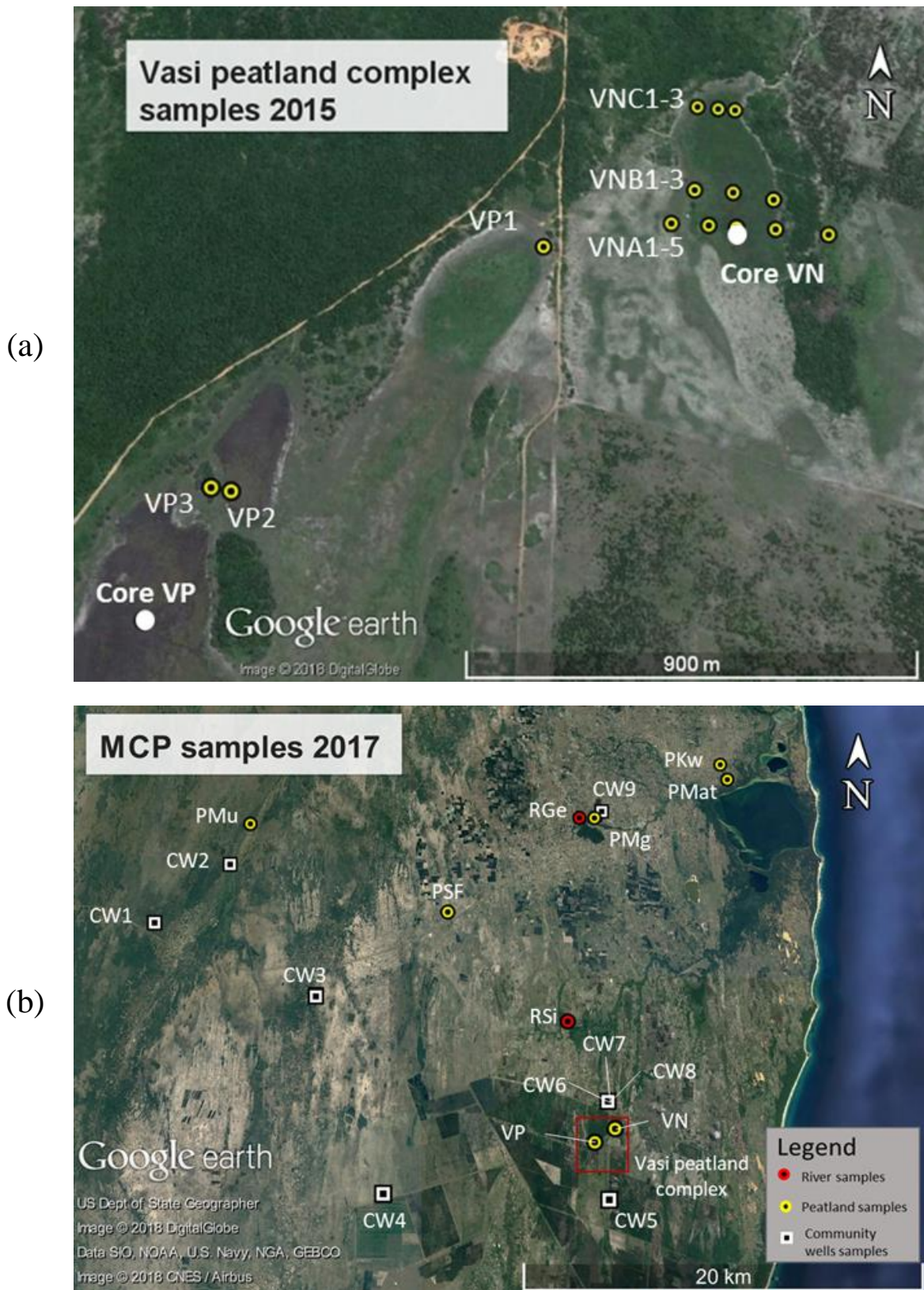
Figure 2. (a) Sampling points (spring 2015) within the Vasi peatland complex (Vasi Pan and Vasi-North) where groundwater tube nests (dipwells and piezometers) were measured and sampled. The white dots indicate the locations of the cores for ^{14}C dating and stratigraphy description. (b) Sampling points in northern Maputaland (MCP) during autumn 2017 from (i) river samples: RSi = Siyadla river, RGe = Gezisa river; (ii) peatlands: PMu = Muzi, PSF = Subsistence farming, VP = Vasi Pan, VN = Vasi North, PMg = Manguzi forest spring, PKw = KwaMbonambe, PMat = Matitimani; and (iii) community wells (CW).

bottoms of the tubes). Groundwater was also sampled in the piezometers, for measurement of δ^2H and $\delta^{18}O$ isotopic content and ionic composition of the water. We sampled the water twice, first in March and again in April after a 5-mm rainfall event. Four other piezometers were added in Vasi-North: three tubes making Transect VNC and a shallow piezometer in the peat layer at Transect VNA (VNA4P1). There were eight observation points in the Vasi peatland complex (Figure 2a), with each point including several piezometers (a total of 17) in the peat and sand layers (details provided later). The observation points were aligned in two west–east transects in Vasi-North (VNA and VNB), following the same direction as the regional groundwater flow in the Maputaland Coastal Plain, and three separate points in Vasi Pan. The VNA and VNB transects were positioned in the thickest part of the Vasi-North peat layer. The transect connecting Vasi Pan and Vasi-North is referred to hereafter as the 'main transect'.

Wider-scale context study (spring 2017)
The second, wider-scale context study took place in spring 2017 (18–25 October) at the end of a dry period, when water levels in the peat were very low. Peat fires had broken out before the field campaign, burning all the peatlands in the Vasi Peatland Complex including Vasi-North. The layout of the 2017 campaign was designed to investigate the relationship between the (local) groundwater systems in Vasi peatland complex and the primary (regional) groundwater system of the Maputaland Coastal Plain.

Despite the increased number of sampling sites, only 18 samples were collected during this campaign, because several tubes fell dry or were lost due to fires. The water samples came from the following areas: (i) areas to the west of Vasi peatland complex (e.g. the Muzi system, which is partly in Tembe Elephant Park; Community Wells 1–3), (ii) areas from the north of Maputaland Coastal Plain (e.g. Manguzi Forest, the Matitimani and KwaMbazambane peatlands and the Gezisa river), and (iii) areas within, and in the surroundings of, the Vasi peatland complex (e.g. Community Wells 4–6 and the Siyadla river). The samples collected during this campaign were analysed for their ^{14}C, $\delta^{13}C$, δ^2H and $\delta^{18}O$ isotopic contents and ion composition (see later for details of laboratory analyses). Four community wells nearby were included, hence the total number of samples was 21. A rainwater sample was taken from the raingauge at location CW6 in 2017. The sampling points and their tube types, depths and diameters of the piezometers and dipwells, along with the sediment type, are listed in Table A1 in the Appendix.

Analysis and interpretation of ionic and isotope data
Ionic composition was used to indicate the origins and flow directions of the groundwater. The samples were first grouped using principal component analysis (PCA) to correlate and cluster water samples with similar ion compositions (and thus identify similar water types), then tracers were used to identify groundwater flow directions. The ionic composition of the samples was checked for ion balance (Appelo & Postma 2005). Chloride and sulphate were used as tracers to identify internal water flows within the Vasi-North basin. Chloride concentrations were used to determine flow directions, based on the assumption that they would increase along the flowline by leaching over the sediments or due to evaporation (Appelo & Postma 2005). Sulphates were used as indicators of anoxic discharge zones (Appelo & Postma 2005).

In order to identify groundwater from different sources, 13 ions were analysed using PCA. We used the "Factoextra" package in "R", which is intended for multivariate statistical analyses including PCA (Kassambara 2017). The outcome was visualised as a plot of 13 variable loadings (ion type and magnitude of contribution to the principal components) and variation in sample distribution based on the first two principal components.

The stable isotope ratios of hydrogen and oxygen (δ^2H and $\delta^{18}O$) can be used to obtain further insight into the origins of water flows. This is done by plotting the sample data with the global meteoric water line (GMWL: $\delta^2H = 8\ \delta^{18}O + 10$), which indicates evaporation processes if the samples collected along a flowline plot with a slope of 4–5 instead of 8 (Schot & van der Wal 1992, Gat 1996). Isotopic compositions are expressed as 'isotope ratios' (R), which are quotients of rare to abundant species; for example, for the stable isotopes of the element carbon, as:

$$^{13}R\ [CO_2] = [^{13}CO_2]/\ [^{12}CO_2] \qquad [1]$$

Changes in isotope ratios are denoted as δ-values, which reflect deviation from a reference material:

$$\delta = ((R_{measured} - R_{reference})/\ R_{reference}) - 1 \qquad [2]$$

The δ-values are expressed in permil (‰). The reference materials used were the Vienna convention standards Pee Dee Belemnite (V-PDB) for ^{13}C and Standard Mean Ocean Water (V-SMOW) for ^2H and ^{18}O (Mook 2006). For the first campaign, the isotope ratio changes (δ^2H and $\delta^{18}O$) were determined by isotope ratio mass spectrometry (IRMS) at the Centre for Water Resources Research at the University of

KwaZulu-Natal (South Africa). Samples from the second campaign were analysed by IRMS at the Environmental Isotope Laboratory at iThemba LABS (also in South Africa).

Water table depth and hydraulic pressure
To assess current water flows in the basins of the Vasi peatland complex, water table depth and hydraulic heads were measured on a weekly basis for two months (February–July 2015) using dipwells and piezometers at different depths. Most data were collected from Vasi-North, which was the only peatland that did not burn in 2015. Measurement of water levels in Vasi Pan became impossible after April 2015 because the peat started to burn and the measuring stations became inaccessible.

Surface altitude was surveyed at each sampling point, as well as at selected points in the topography, e.g. the tops of ridges, by a private firm (F.J. Loock Land Surveyors) using a differential GPS linked to a base station.

Groundwater tubes: installation and sampling
The holes for the tubes (dipwells and piezometers) were drilled using a hand auger (Ø ~ 50 mm) in the sand layers and a Russian peat corer in the peat layers (Ø ~ 60 mm). The dipwells were made of polyvinyl chloride (PVC) tubing (Ø = 50 mm) and perforated along their entire lengths (0.5 mm per 1 cm), while the piezometers had diameters of 20 and 40 mm (due to limited availability at the local stores) and a 20-cm screen at the bottom. Each groundwater tube was inserted in a separate hole.

Before sampling, all groundwater tubes were flushed using a hand pump to allow the water levels to re-stabilise. Water sampling occurred one to four days after flushing. In some cases, flushing the groundwater tubes was not possible, especially for the community wells. In such cases, ^{14}C samples were not taken, e.g. CW5 in 2017. Water samples were collected using 100-ml PVC bottles for ion composition analyses, 30-ml dark glass bottles for stable isotopes analysis and 500-ml dark glass bottles for carbon isotopes analysis. They were all filled to the brim, with no field filtering or measurements. They were filtered in the relevant laboratory, one to two weeks after sampling, then stored in a refrigerator at 4 °C. A probable consequence of this protocol was that NO_3 concentration would be too high, owing to transformation of NH_4 into NO_3 by microbes.

Water samples for ion composition analysis from both campaigns were sent to the laboratory of the Institute for Soil, Water and Climate in Pretoria (South Africa) where they were filtered, pH was measured, and ion compositions (HCO_3, Cl, SO_4, Ca, Na, Mg, K, SiO_2, Fe, PO_4, NO_3 and NH_4) were determined using ICP-MS (Bos & Fredeen 1989).

Radiocarbon dating of water
Water samples for carbon isotope analysis were collected from the 14 locations (Figure 2b) that yielded enough clean groundwater to completely fill one of the glass sample bottles. The samples were analysed at CIO in The Netherlands. The dissolved inorganic carbon (DIC) was captured via the samples' CO_2 gas and pressed into graphite. After this, activity of the graphite sheets was counted using the accelerator mass spectrometer (AMS) facility. The results were given in percent modern carbon (pMC) relative to a reference material, with the present defined as the year 1950:

$$^{14}Csample = (^{14}C_{measured} / {}^{14}C_{reference}) \, pMC \qquad [3]$$

(Mook 2006). Hence, a sample from a water flow that had infiltrated around 1950 would have ^{14}C = 100 pMC, while the value for a sample that infiltrated earlier would be less than 100 pMC. The δ^{13}C content of the samples was measured using IRMS and was reported as permil (‰). The δ^{13}C values are used in order to exclude ^{14}C values that have been affected by chemical processes (Han *et al.* 2012). The samples with δ^{13}C values outside the range from -11 to -14 ‰ could be have been affected by geochemical processes that would mask the ^{14}C values. For instance, samples with more depleted δ^{13}C values, close to -25 ‰, would be diluted by release of dead organic material (Mook 2006, Han *et al.* 2012).

RESULTS
Peat stratigraphy
Figure 3 shows Vasi-North's stratigraphic profile, with the lowest 5–6 m filled with organic gyttja. On the eastern side of the transect, a gradual change from organic gyttja to peat-gyttja and sedge peat was found. In the western part, however, a peat-gyttja horizon occurred in the sedge peat.

Furthermore, the first 5–6 m from the bottom in the west part consisted of gyttja in which only a few remains of plants were found; amongst them were stem bases of *Cladium mariscus* subsp. *jamaicense*, which grows in shallow water. Above the gyttja layer (at 182–128 cm), well-preserved (H4–H6) radicell peat was found containing remnants of rhizomes of *Cladium mariscus* subsp. *jamaicense* and seeds of
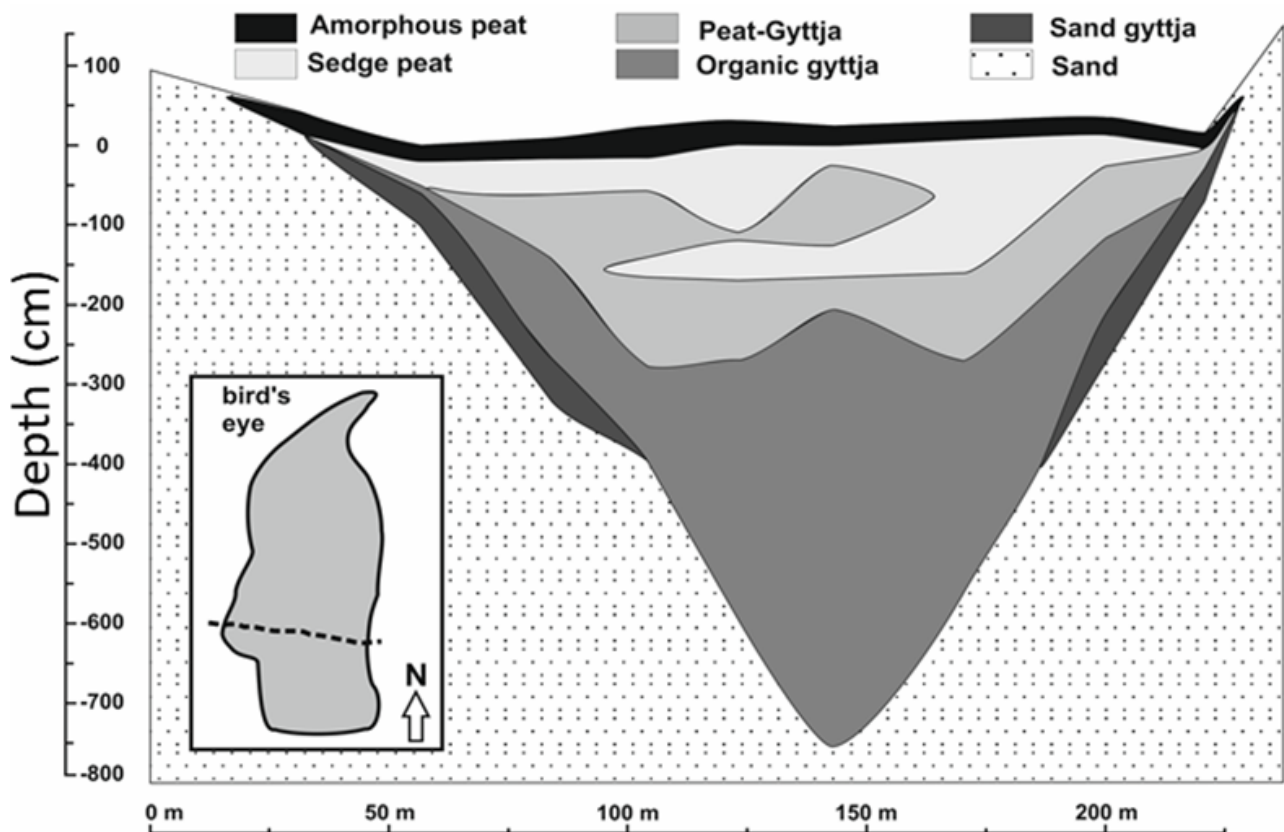
Figure 3. Detailed stratigraphy of the deposits in Vasi-North, which was described from five cores spaced approximately 50 m apart. The small map (left) shows the position of the transect in the peatland.

Eleocharis dulcis. The deposit at 128–94 cm was composed of peat-gyttja. At 94 cm, there was again a shift to radicell peat and a decline of gyttja. The topsoil of the whole peatland consisted of amorphous peat, with soil aggregates and cracks mostly in the uppermost 10–20 cm.

^{14}C dating and accumulation rates

Table 1 lists the results of ^{14}C dating the stratigraphic layers and calculations of accumulation rate. Organic matter accumulation in the Vasi peatland complex started with the gyttja layer in the Vasi-North basin, dated at 8490 calBP. In Vasi Pan, gyttja accumulation started around 3900 calBP. The periods of gyttja accumulation were characterised by relatively low accumulation rates (0.4–0.6 mm yr^{-1}). On the other hand, fibrous sedge peat had started to accumulate in Vasi Pan by 2800 calBP, when the lower lying Vasi-North basin was still accumulating peat-gyttja. The radiocarbon ages of the present top layer (about 40 cm below surface) of Vasi Pan and Vasi-North were about 2400 and 1965 calBP, respectively. The average accumulation rate for the peat was around 1.5 mm yr^{-1} with a maximum of 4 mm yr^{-1} during the period from 2900 to 2700 calBP in Vasi Pan.

Origin of groundwater flow

Water table depth and hydraulic head

Regular readings of groundwater levels are presented in Table A4. Measurements are available for Vasi-North (only) because all other peatlands in the complex burned in 2015. The data show that the water table was high only in spring 2015. The deepest piezometers (at VNA3) indicated exfiltration of groundwater until June 2015. After that all available piezometers indicated infiltration conditions and water levels dropped steadily. The record from Station VNA5, situated to the east of Vasi-North and outside the mire itself, shows that the mire was possibly losing water to the east during the whole of the observation period.

The surface altitudes and water table depths measured on 24 March 2015, from SW to NE along the main transect across Vasi Pan and Vasi-North, are shown in Figure 4. The average altitudes of the basin surfaces decreased from around 56 m a.m.s.l. at Vasi Pan to 54 m at Vasi-North. The bordering sand ridges ranged in width from 150 m to 300 m and reached a height of 3–5 m above the surfaces of the peatlands (58–60 m a.m.s.l.), with the widest ridge separating

Table 1. List of the measured radiocarbon dates in BP for the peat samples, the $\delta^{13}C$ values, and the calibrated date range (in calBP, calendar years relative to 1950 AD). The ^{14}C values were rounded to the nearest 5 calBP. Accumulation rates were calculated using the difference in age per difference in depth.

| Site	Depth (m)	Depth (m a.m.s.l.)	Lab no. (GrA)	Sample description (von Post H)	^{14}C (BP)	Calibrated age range (calBP, 1σ)	$\delta^{13}C$ (‰)	Accum. rate (mm yr^{-1})
Vasi-North	0.47	53.32	63234	Amorphous peat (H10)	2045 ±30	1930–2000	-16.65	1.15
	0.94	52.85	63236	Radicell peat (H4-H5)	2385 ±30	2325–2425	-20.72	0.63
	1.28	52.51	63237	Peat-gyttja (H6)	2890 ±35	2880–3005	-24.14	1.75
	1.82	51.97	63238	Radicell peat (H4-H5)	3050 ±35	3080–3325	-26.17	1.51
	2.14	51.65	63239	Gyttja	3230 ±35	3375–3450	-23.57	1.25
	5.16	48.63	63240	Gyttja with high water content	5105 ±40	5750–5890	-19.83	1.09
	8.05	45.74	63241	Gyttja bottom (underlain by sand)	7760 ±45	8435–8545	-17.76	-
Vasi Pan	0.4	56.68	63242	Amorphous peat (H10)	2420 ±30	2345–2455	-19.77	0.48
	0.65	56.43	63243	Fibrous peat (H3)	2745 ±30	2765–2845	-20.27	4.39
	1.01	56.07	63264	Gyttja	2820 ±35	2795–2930	-25.11	0.39
	1.42	55.66	63247	Gyttja bottom (underlain by sand)	3660 ±35	3870–3980	-22.32	-
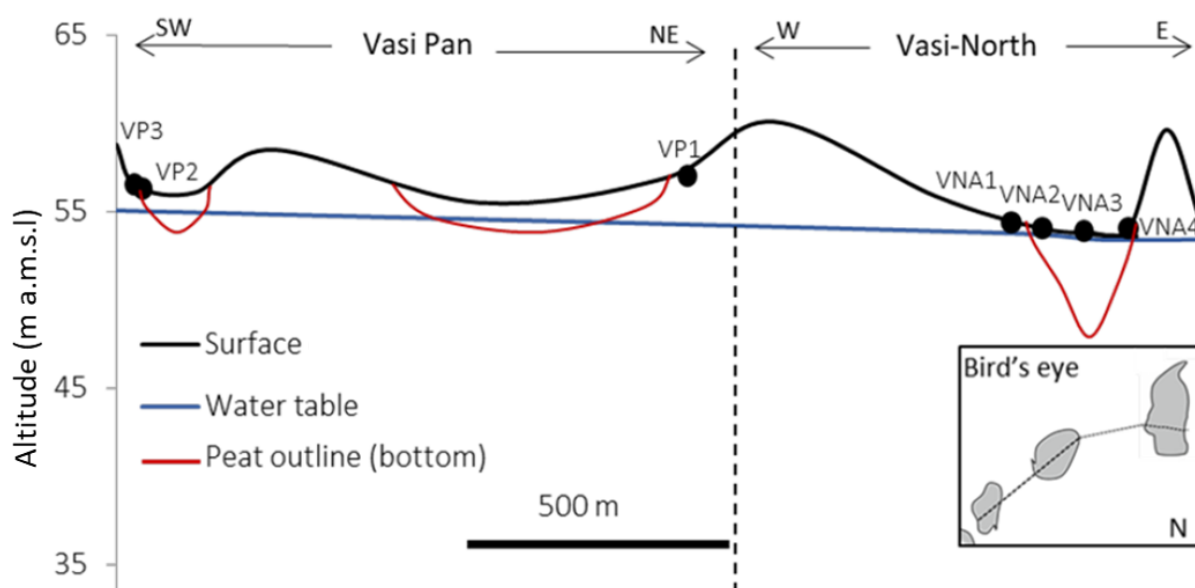
Figure 4. Topographic relief (black line) and water table depth (blue line) along a transect (main transect) extending through Vasi Pan (0–1200 m, SW to NE direction) and Vasi-North (1200–2000 m, W to E direction); water table depth was measured on 24 March 2015.

Vasi Pan from Vasi-North. Water table level also decreased along the transect from Vasi Pan to Vasi-North during the measurement period February–July 2015.

At Vasi-North, the hydraulic head of the water table in the mineral soil at the western side was 0.05 m greater than in the peat layer. However, at the eastern side the hydraulic head of the water table in the mineral layer was about 0.21 m less than in the peat layer. This indicates a potential upward flow of groundwater at the western side of the pan and a downward flow at the eastern side (Figure 5).

Ion compositions and tracers
PCA results of the water's ion composition are shown in Figure 6. These results are expressed in a plot of the first two principal components (PC1 and PC2). PC1 explained 40.5 % of the variation, while PC2 explained 22.2 %. To facilitate interpretation, the PCA results were divided into two components: (a) the ion variables and their contributions to PC1 and PC2, and (b) the correlations of samples to PC1 and PC2. The contributions of ion concentration to the principal components are expressed in both arrow length and colour. The directions of the arrows indicate the qualitative relationship between ion content and the principal components. For example, SO_4 and Fe ions are directly proportional to PC1 and inversely proportional to PC2, which means samples with higher SO_4 and Fe ions content are likely to be found in the quadrant with positive values for PC1 and negative values for PC2.

PCA indicated four groups with respect to ion composition. Group A, located in the negative quadrant of Figure 6, has the most samples. Characterised by generally low ion content, Group A also contains the rainwater sample taken in 2017, along with all samples from the community wells except for CW1 and CW2, the Siyadla river samples, some of the Vasi Pan samples, and samples from the southwestern parts of Vasi-North (Samples 5 and 7). Group B contains samples directly proportional to PC1, with higher SO_4, NH_4, Mg, Na and Cl content. Most of the samples in Group B originate from the central and eastern parts of Vasi-North. They showed especially high SO_4 content (except for 8, 10 and 26), with the highest values in Sample 16 from VNB3 (west of Vasi-North). Group C, with higher HCO_3, SiO_2 and PO_4, contains Samples 27 and 37, which are from two peatlands in the northern part of MCP (the spring in Manguzi forest and KwaMazambane).

For a closer look at the spatial distribution of ion composition in the groundwater, Figures 7a and 7b show the W–E Transect A in Vasi-North, with profiles of chloride and sulphate concentrations in the groundwater. These ion gradients show an increasing trend towards the east, but the highest concentrations were found in the central part of the basin. The
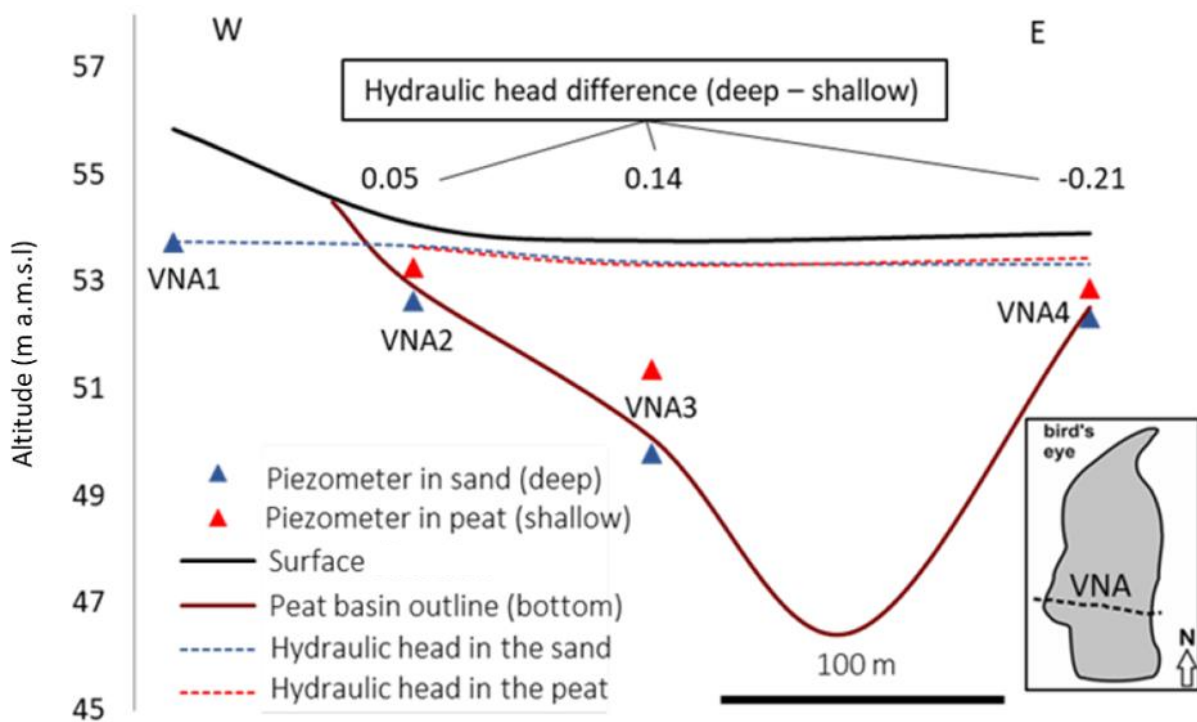

Figure 5. Hydraulic heads in the organic layer (blue dashed line) and the mineral layer (red dashed line) along Transect A, west to east direction, in Vasi-North.

1	Rsi	16	VNB3P	31	CW9Rain
2	VP1	17	VNB3W	32	CW4
3	VP2	18	CW5	33	CW5*
4	VP3	19	CW7	34	CW6*
5	VNA1P	20	CW8	35	VP3*
6	VNA2W	21	CW6	36	VN
7	VNA2P2	22	CW2	37	PKw
8	VNA3P1	23	CW1	38	Rsi*
9	VNA3W	24	CW3a		
10	VNA3P2	25	CW3b		
11	VNA4P2	26	PSF		
12	VNA5	27	PMg		
13	VNB1P	28	PMat		
14	VNB1W	29	RGe		
15	VNB2W	30	CW9		
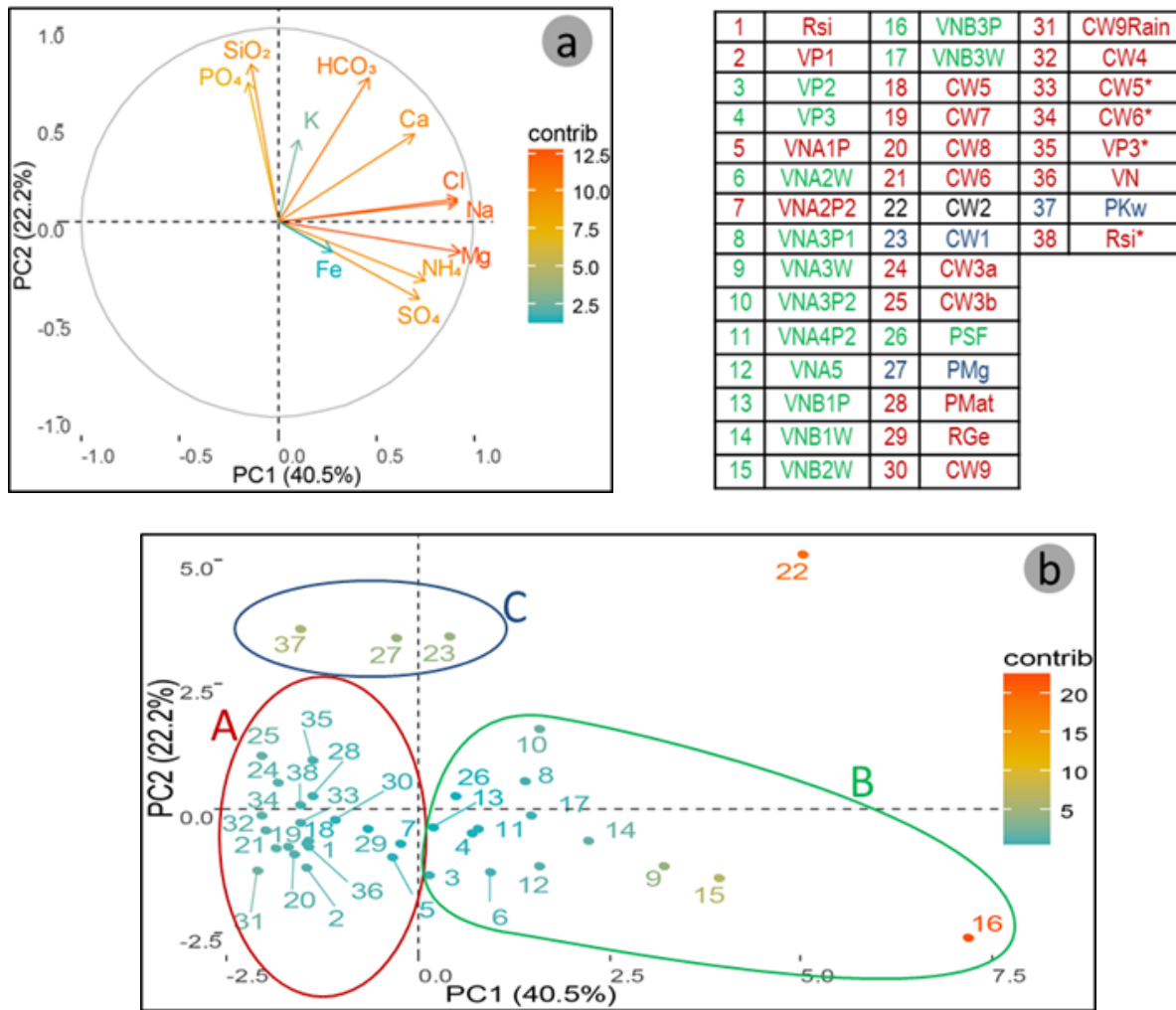
Figure 6. PCA of water ion composition based on the first two principal components (PC1 and PC2): (a) the contribution of variables (ions) to the first two PCs, where arrow length indicates the magnitude and arrow direction indicates which PC axis received the greatest contribution; (b) the distribution of the samples along PC1 and PC2, where the axis units express the magnitude of variation along the principal component.

Figure 7. Distribution of the groundwater solute tracers along Transect A in Vasi-North: (a) chloride and (b) sulphate. Lines to the right of the white bar are interpolated, extending across the (unsampled) western side of the basin to the single sampling point at VNA4.

sulphate ion gradient shows a possible anoxic pocket at VNA3 at 4 m depth. The full results of the ion composition of the water samples is shown in Tables A2 and A3.

δ¹⁸O and δ²H stable isotopes
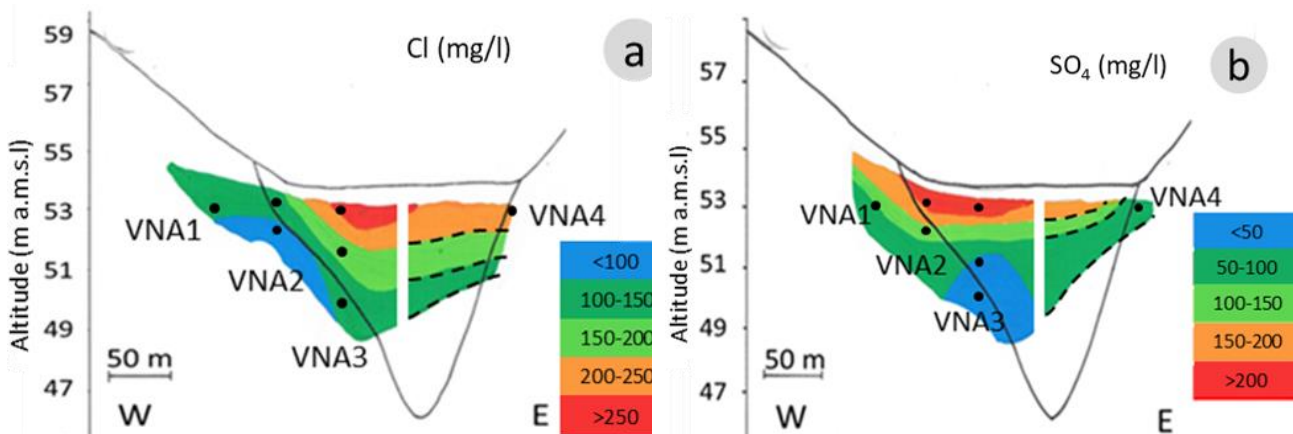The stable isotopes results are plotted with the GMWL for: (i) the first field campaign, in the Vasi area, which included two rounds of sampling: before and after a 5-mm rainfall event (Figures 8a and 8b, respectively) and (ii) the larger-scale second field campaign with the samples covering MCP (Figure 9).

The samples from the sand layer in the western parts of Vasi-North (A1, A2P2 and B1P) are shown to have isotopic content similar to the community

well samples (Figure 8a). Sample A5, which was taken from the basin to the east of Vasi-North, had similar values. Most of the peat water samples had $\delta^{18}O$ values > -2 ‰ (e.g. A2W, A3W, A3P1, B1W and B3W). Some samples (e.g. B3P, B1W, CW5) had values indicating evaporation processes, i.e. below GMWL.

After the rainfall event (Figure 8b), the isotopic values of all samples had shifted above the GMWL, except for Sample A4P2 (west of Vasi-North). Despite this, the samples with $\delta^{18}O$ values > -2 ‰ remained more or less the same. It appears that the local meteoric water line (LMWL) would plot well above the GMWL with a deuterium excess of close to -15 ‰.
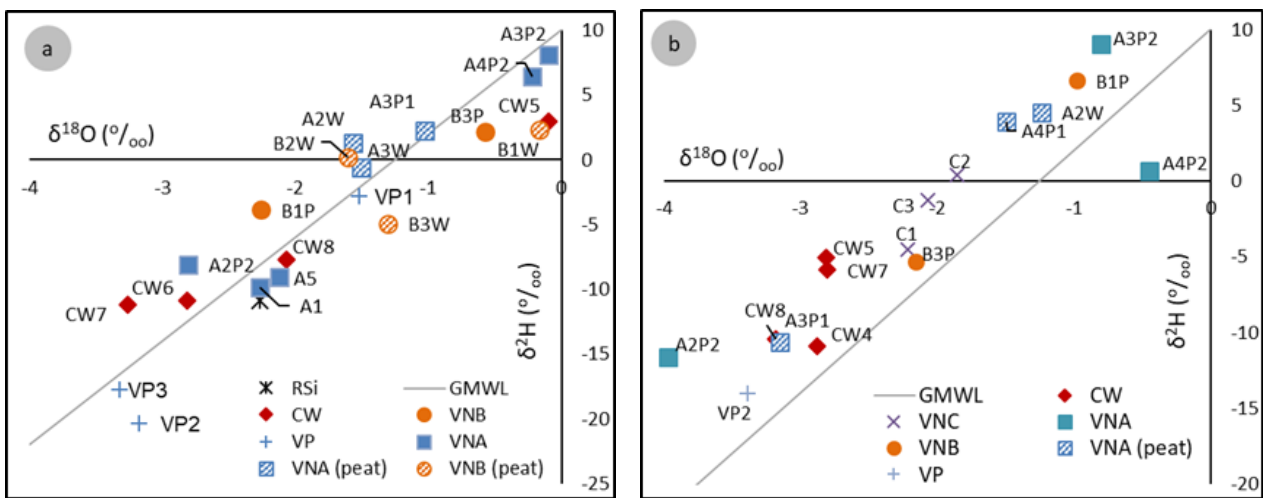

Figure 8. (a) Isotopic compositions of the water samples from the Vasi peatland complex in March 2015. (b) Isotopic compositions of the water samples taken in April 2015 after a 5-mm rainfall event. The VNC transect was measured only in April.
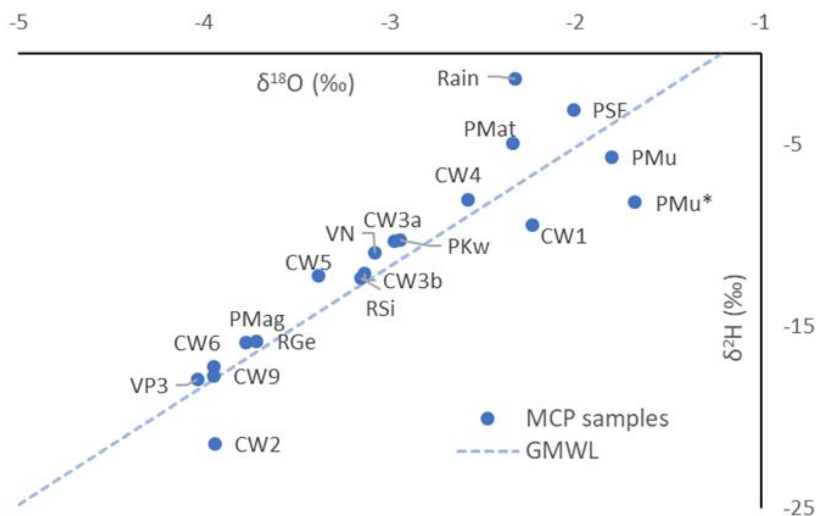

Figure 9. Stable isotopes content in water samples from the second campaign covering the northern part of the Maputaland Coastal Plain.

Figure 9 shows that most samples from the regional groundwater (community wells and river water), as well as the rainwater from October 2017, had $\delta^{18}O$ values $>$-2 ‰. The Muzi system and the nearby community wells in Tembe Elephant Park were the only locations where isotopic contents shifted below the GMWL. Figure 8a shows that most of the water samples had different isotopic values in the second sampling round, with the exception of those from community wells with $\delta^{18}O$ values $<$-2 ‰ (CW6, CW7, CW8).

Groundwater ^{14}C dating
Table 2 lists the results of the carbon isotope analysis. Most of the samples appeared to be within the range of current infiltration or infiltration during the past 60 years (post 1950, above or close to 100 pMC). The lowest ^{14}C results were observed near the Muzi system (PMu, CW1 and CW2). Some samples from the peatlands indicated a shift towards enrichment by dead organic matter, which is indicated by lower $\delta^{13}C$ values (e.g. VN, VP3, PMat, RGe). This was also the case for community wells near the Vasi peatland complex (e.g. CW4, CW6).

DISCUSSION

Peat development and past hydrological conditions

The peatlands in the Vasi peatland complex are typical examples of terrestrialising peatlands (Heathwaite *et al.* 1993). Vasi-North, the lowest lying basin in the complex, contained an open lake accumulating gyttja during the Early-Holocene, around 8850 calBP. The persistent accumulation of organic matter over millennia seems to have dominated most of Vasi-North's developmental pathway. The timeline of gyttja layer initiation in the basins of the complex indicates that infilling of Vasi-North may have created a positive feedback that triggered peat accumulation in the Vasi Pan basins - the lower-permeability gyttja and peat layers in Vasi-North acting as obstructions to water flow and thus raising the water table in the higher parts of the complex, i.e. Vasi Pan. Similar observations have been made for the nearby Mfabeni and Matitimani peatlands (P. Grundling *et al.* 2013, Gabriel *et al.* 2017). This may also explain, in turn, why the lower-altitude Vasi-North peatland became degraded last in

Table 2. ^{14}C dating of 14 groundwater samples in the northern part of the Maputaland Coastal Plain.

No.	Code	Lab. No. (GrM)	^{14}C uncorrected (pMC)	±	$\delta^{13}C$ (‰; IRMS)	±
1	Pmu	11527	75.71	0.15	-12.71	0.15
2	CW2	11528	71.71	0.15	-12.63	0.15
3	CW1	11529	51.2	0.12	-9.51	0.15
4	CW3a	11530	102.48	0.31	-13.26	0.15
5	CW3b	11532	98.12	0.18	-8.49	0.15
6	PSF	11534	107.3	0.19	-12.45	0.15
7	PMag	11535	98.06	0.18	-11.20	0.15
8	PMat	11537	97.89	0.18	-16.30	0.15
9	RGe	11538	100.57	0.19	-19.35	0.15
10	CW9	11539	108.36	0.19	-19.73	0.15
11	CW6	11540	108.75	0.19	-17.13	0.15
12	CW4	11542	115.91	0.20	-17.84	0.15
13	VA3	11544	87.52	0.17	-19.53	0.15
14	VN	11545	99.56	0.18	-20.09	0.15

the sequence, after the peatlands in Vasi Pan; degradation spread from one basin to another in an inverse timeline to that of initiation, consistent with the altitudinal sequence of the basins.

While the Vasi peatland complex might be in a separate hydrological catchment from other peatlands in the Maputaland coastal plain, the climatic conditions over recent millennia seem to be similar or at least with no large deviations. The average peat accumulation rate (mean around 1.5 mm yr^{-1} with a maximum of 4 mm yr^{-1} for the period 2900–2700 calBP) is consistent with estimates from older peat dating studies in Maputaland, which yielded values no higher than 2.5 mm (Thamm *et al.* 1996, Page *et al.* 2004, Baker *et al.* 2014).

Local versus regional groundwater systems

Dating indicates that the groundwater in the Vasi peatland complex and its surrounding dunes is relatively recent (young groundwater), suggesting that the water originates from local groundwater systems. This is also the case for most of the groundwater discharging to the other wetlands in the northern Maputaland coastal plain. Most of the radiocarbon data had values near 100 pMC, which is due to the bomb peak in 1950 (Mook 2006). The source of these flows is likely to be either from the KwaMbonambi Formation or the Kosi Bay Formation and also likely to be limited to localised catchments (Weitz & Demlie 2014, Kelbe *et al.* 2016). Only groundwater in the Muzi system is relatively (up to a few hundred years) old; i.e. this system seems to be under the influence of groundwater discharging from the Uloa Formation (Weitz & Demlie 2014), which was also evident from the water's ion composition (>1000 mg L^{-1}). The ion composition of the groundwater discharging at Vasi peatland complex indicates consistent similarity with groundwater feeding other peatlands in the north-eastern part of the Maputaland coastal plain (Bate *et al.* 2016). The stable isotopes content of groundwater at the western side of the Vasi-North basin was also similar to that observed in groundwater samples from other locations on the Maputaland Coastal Plain, except for the groundwater in the Muzi system.

The difference in groundwater source for the upstream area (i.e. Muzi system) from the middle (i.e. Vasi peatland complex) and the downstream (i.e. Matitimani and KwaMbazambane) peatlands could be due to formation of nested local to intermediate groundwater systems in the Kosi Bay and KwaMbonambi formations on top of the regional system in the Uloa Formation. Some of these local systems could be perched due to the presence of iron-rich sand deposits at greater depths (Botha & Porat

2007, Kelbe *et al.* 2016). Toth (1963) has shown that such local systems could also be nested within a gently sloping regional aquifer, which is the case in the Maputaland Coastal Plain. Kelbe *et al.* (2016) indicated that such layering of groundwater systems could exist, but was one of the limitations within their constructed groundwater model, and would require more information.

An important finding is that the initiation of peat accumulation in Vasi peatland complex, ca. 9000 calBP, is earlier than the peak of peat initiation in the other in Maputaland peatlands. For instance, Grundling (2004) has indicated that the peatland initiation peak in the Maputaland Coastal Plain coincides with the sea level rise peak ca. 4000 years ago. Also, the peat initiation in Matitimani is substantially younger (ca. 6000 calBP, see Gabriel *et al.* 2017) than in the Vasi peatland complex. This is an indication that the Vasi peatland complex is independent of the groundwater systems supplying other peatlands in the lower parts of the Maputaland Coastal Plain. A more likely scenario is that the Vasi peatland complex is supplied by a perched aquifer within the KwaMbonambi Formation. It would also mean that we can separate the local to intermediate system of the Kosi Bay and KwaMbonambi Formations into intermediate and local systems, respectively.

Hydrological system of Vasi peatland complex

Notably within the Vasi peatland complex, the water table showed a gradient that was independent of the topographic highs (dune ridges). However, it followed the gradient of the peat surface in the basins, where water table depth increased from Vasi Pan to Vasi-North. This indicates a possible cascading system where the groundwater flows from one basin to the next along the altitude gradient. This was also observed in other peatland systems, e.g. the Mfabeni mire in the south of Maputaland Coastal Plain (Grundling 2014) and a small mire near the High Tatra Mountains in Slovakia (Grootjans *et al.* 2006). The concept of throughflow wetlands was introduced by Stuyfzand (1993) in the coastal dunes of The Netherlands. His conceptual model suggested discharge of groundwater (inflow) on one side of the dune slack and recharge (outflow) on the other side. The hydraulic head data from Vasi-North indeed indicate groundwater discharge into the southwestern edges of the basin at VNA2 and VNA3 and out from the basin at the opposite side.

It is noted that, under long-lasting dry conditions, the change in chemical composition of the discharging groundwater is possibly related to processes occurring within the peat basin, e.g.

oxidation and evaporation (Naucke *et al*. 1993), which then cascades from one basin to the next. Synthesising the water table depth and tracer data, it seems that the Vasi peatland complex functions as an inter-dune cascading system with throughflow systems within the basins. Figure 10 shows a conceptual model of the groundwater discharge zones in Vasi-North, the throughflow directions and the hypothetical connection to the Vasi Pan basins (van Loon *et al*. 2009).

Synthesis and reflection on degradation cause
Despite the existing groundwater discharge to Vasi-North during the wet season, the water table was dropping steadily during the study period from January 2014 up to the end of the wet season in April 2015 (Table A4). Specifically, the groundwater table dropped to more than 50 cm below the surface on the eastern side of Vasi-North. Most of the dipwells (< 1 m deep) within the peat layer were dry by April 2015. Meanwhile, the water table depth at Vasi Pan dropped to more than 1.5 m below the surface of the peat layer (at VP2), while VP1 was dry. Furthermore, the top layers in the Vasi peatland complex are highly degraded (see Table 1). The radiocarbon ages of the bottoms of the amorphous organic top layers of Vasi Pan and Vasi-North were about 2400 and 1965 calBP respectively, indicating that most of the accumulations younger than ca. 2000 years have disappeared due to peat oxidation, burning and wind erosion. Moreover, the macrofossil analysis of peat profiles indicated the effects of wet and dry periods.

Gabriel *et al*. (2017), working in other peatlands nearby, also found evidence for the occurrence of dry conditions causing natural fires, in the form of microcharcoal fossils. However, the profile did not indicate degradation of lower layers resulting from the occurrence of long-persisting dry periods; this was observed only for the top layer. Also, no evidence was found for loss of peat to intensive fires in the past; we did not detect any considerable discontinuities in peat age from initiation at 8850 calBP until the most recent date at 1950 calBP. Lastly, the order of basin degradation, i.e. the higher Vasi Pan degrading first followed by Vasi-North, suggests a gradual yet persistent lowering of the groundwater table.

Hence, persistent lowering of the groundwater table does not seem to have been a natural characteristic of the Vasi peatland complex under past hydrological conditions. It could be similar to the situation in the Mbazwana catchment, south of the Vasi peatland complex, where simulations of water table drawdown appeared to be affected more by the difference in evapotranspiration between treed areas (plantations and woodlots) and natural grasslands (see Bate *et al.* 2016). Also, Grundling & Blackmore (1998) reported fast recovery of the water table in 1998, after plantations were cleared from the Vasi-North basin.

Thus, our research supports the results of hydrological modelling by Kelbe *et al*. (2016) and Bate *et al*. 2016, who studied the effects of pine and blue gum plantations on hydrology in the
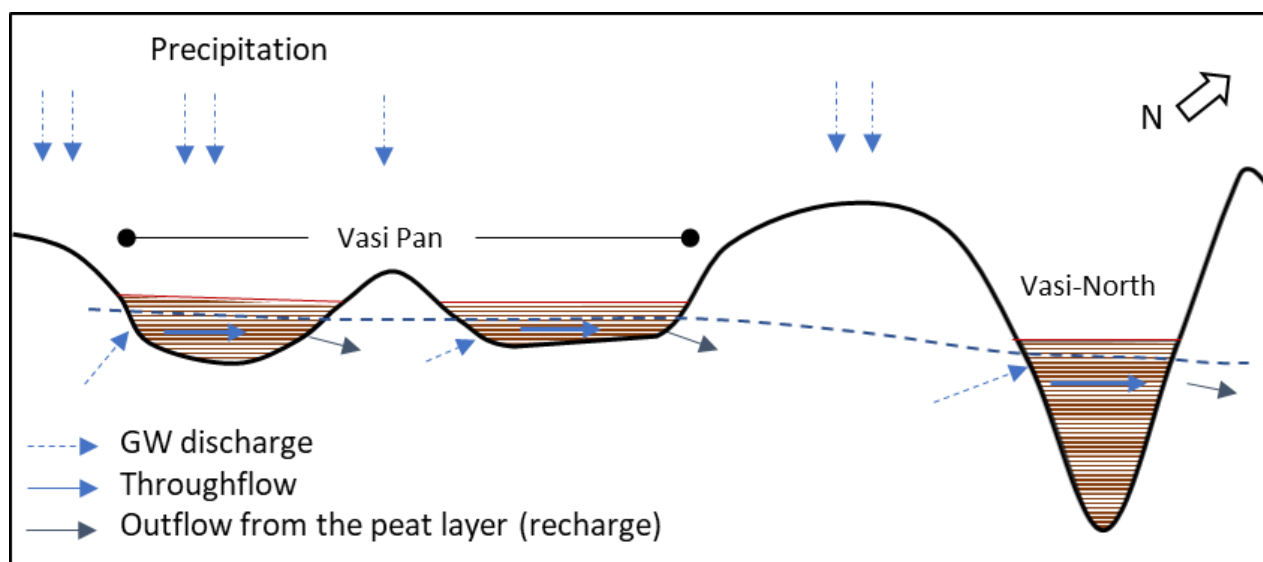

Figure 10. Conceptual model of the hydrological system of the Vasi peatland complex. Dashed blue lines represent discharge of groundwater (inflow), light blue lines indicate hypothetical throughflow within the peatland, and dark blue lines represent recharge from the peat (outflow) into the adjacent dune at the opposite side of the wetland.

Mgobezeleni catchment area near the town of Mbazwana, to the south of our research area. They concluded that groundwater tables have dropped due to the dry climate cycle (see A.T. Grundling *et al.* 2013) but also, more importantly, due to groundwater interception and evapotranspiration in the commercial plantations. The extreme degradation of the Vasi peatlands and the persistent lowering of the water table appears to be a reflection of changes in external landscape management, which were enhanced by the last dry climate cycle. The possible losses of ecosystem services provided by the Vasi peatland complex, e.g. CO_2 sequestration, local subsistence activities (e.g. grazing, gardening) are not yet known, but are considerable because all of the peat basins in our study area have now been burned to a depth of approximately 30 cm. Following the suggestions expressed by Grundling & Blackmore (1998) almost 20 years ago, we also emphasise the need for an effective water management plan that regulates and restricts further continuation of the presently intensive forestry practices.

To this end, the possible drawdown cone resulting from the plantation area needs to be quantified in order to plan a rationalised buffer zone that protects the groundwater supply to the peatland. A groundwater monitoring project is currently being carried out in the Vasi peatlands in order to record the effects of future land use changes. Furthermore, the best options for restoring the severely desiccated, burned and unvegetated peatlands with salt-encrusted surface layers should be studied in more detail.
.

AUTHOR CONTRIBUTIONS

Hydrological field data were collected by SE, SB, PG, LP and APG. MB analysed the stable isotopes (δ^2H and δ^{18}O). MG carried out the detailed stratigraphy of Vasi-North, while JVdP supervised the work on carbon dating of soil and groundwater. APG and PG did the overall supervision of the project.

REFERENCES

Aerts, A.T., van der Plicht, J. & Meijer, H.A.J. (2001) Automatic AMS sample combustion and CO_2 collection. *Radiocarbon*, 43(2), 293–298.

Appelo, C.A.J. & Postma, D. (2005) *Geochemistry, Groundwater and Pollution*. Second edition, A.A. Balkema Publishers, Leiden, 595 pp.

Baker, A., Routh, J., Blaauw, M. & Roychoudhury, A.N. (2014) Geochemical records of palaeoenvironmental controls on peat forming processes in the Mfabeni peatland, Kwazulu-Natal, South Africa since the Late Pleistocene. *Palaeogeography, Palaeoclimatology, Palaeoecology,* 395, 95–106.

Bate, G., Kelbe, B.E. & Taylor, R. (2016) *Mgobezeleni, the Linkages Between Hydrological and Ecological Drivers*. Report No. K5/2259/1/1, Water Research Commission (WRC), Pretoria, 225 pp.

Bos, C.B. & Fredeen, K.J. (1989) *Concepts Instrumentation and Techniques in Inductively Coupled Plasma Atomic Emission Spectroscopy*. Perkin-Elmer Cooperation, Norwalk, 120 pp.

Botha, G. & Porat, N. (2007) Soil chronosequence development in dunes on the southeast African coastal plain, Maputaland, South Africa. *Quaternary International*, 162–163, 111–132.

Botha, G.A., Bristow, C.S., Porat, N., Dullerj, G., Clarkei, B. M., Armitagej, S.J. & Schoemani, P. (2003) Evidence for dune reactivation from GPR profiles on the Maputaland Coastal Plain, South Africa. In: Bristow, C.S. & Jol, H.M. (eds.) *Ground Penetrating Radar in Sediments*, Special Publication, Geological Society of London, UK, 29–46.

Botha, G., Haldorsen, S. & Porat, N. (2013) Geological history. In: Perissinotto, R., Stretch, D.D. & Taylor, R.H. (eds.) *Ecology and Conservation of Estuarine Ecosystems: Lake St Lucia as a Global Model.* Cambridge University Press, Cambridge, UK, 47–62.

Bronk Ramsey, C. (2009). Bayesian analysis of radiocarbon dates. *Radiocarbon*, 51(1), 337–360.

Bruton, M.N. (1980) An outline of the ecology of the Mgobezeleni Lake System at Sodwana, with emphasis on the Mangrove Community. In: Bruton, M.N. & Cooper, K.H. (eds.) *Studies on the Ecology of Maputaland*, Cape and Transvaal Printers, Cape Town, 408–426.

Gabriel, M., Gałka, M., Pretorius, M.L. & Zeitz, J. (2017) The development pathways of two peatlands in South Africa over the last 6200 years: implications for peat formation and palaeoclimatic research. *The Holocene*, 27(10),

1499–1515.

Gabriel, M., Toader, C., Faul, F., Roßkopf, N., van Husyssteen, W.C., Grundling, P.L. & Zeitz, J. (2018) Peatland substrates in northern KwaZulu-Natal: Their forming environments, their properties and an approach towards their classification. *South African Journal of Plant and Soil*, 35, 149–160.

Gat, J.R. (1996) Oxygen and hydrogen isotopes in the hydrologic cycle. *Earth Planet Sciences*, 24, 225–262.

Grootjans, A.P. & Jansen, A. (2012) An eco-hydrological approach to wetland restoration. In: Grootjans, A.P., Stanova, V.S. & Jansen, A.J.M. (eds.) *Calcareous Mires of Slovakia*, KNNV Publishing, Zeist, 21–28.

Grootjans, A.P., Adema, E.B., Bleuten, W., Joosten H., Madaras, M. & Janakova, M. (2006) Hydrological landscape settings of base-rich fen mires and fen meadows: an overview. *Applied Vegetation Science,* 9, 175–184.

Grootjans, A.P. & van Diggelen, R. (2009) Hydrological dynamics III: Hydro-ecology. In: Maltby, E. & Barker, T. (eds.) *The Wetlands Handbook*, Wiley/Blackwell, Chichester, 194–212.

Grundling, A.T. (2014) *Remote Sensing and Biophysical Monitoring of Vegetation, Terrain Attributes and Hydrology to Map, Characterise and Classify Wetlands of the Maputaland Coastal Plain, KwaZulu-Natal, South Africa*. PhD thesis, University of Waterloo, Canada, 156 pp.

Grundling A.T., van den Berg, E.C. & Price, J.S. (2013) Assessing the distribution of wetlands over wet and dry periods and land-use change on Maputaland Coastal Plain, north-eastern KwaZulu-Natal, South Africa. *South African Journal of Geomatics*, 2(2), 120–139.

Grundling, P. (2004) The role of sea-level rise in the formation of peatlands in Maputaland. In: *Boletim Geológico 43*, Ministerio dos Recursos Minerais e Energia, Direccao Geral de Geologia Mozambique, 58–67.

Grundling, P. & Blackmore, A. (1998) *Peat Fire in the Vasi Pan Peatland: Manzenwenya Plantation*. Report No. 1998-0208, Council of Geoscience, Pretoria, 47 pp.

Grundling, P. & Grobler, R. (2005) Peatlands and mires of South Africa. *Stapfia,* 85, 379–396.

Grundling, P., Mazus, H. & Baartman, L. (1998) *Peat Resources in Northern KwaZulu-Natal Wetlands: Maputaland*. Report No. A25/13/2/7, Department of Environmental Affairs and Tourism, Pretoria, 102 pp.

Grundling, P., Baartman, L., Mazus, H. & Blackmore, A. (2000) *Peat Resources of KwaZulu-Natal Wetlands: Southern Maputaland and the North and South Coast*. Council for Geoscience Report 2000-0132, Department of Environmental Affairs and Tourism, Pretoria, 120 pp.

Grundling, P., Grootjans, A.P., Price, J.S. & Ellery, W.N. (2013) Development and persistence of an African mire: How the oldest South African fen has survived in a marginal climate. *Catena*, 110, 176–183.

Han, L.F., Plummer, L.N. & Aggarwal, P. (2012) A graphical method to evaluate predominant geochemical processes occurring in groundwater systems for radiocarbon dating. *Chemical Geology*, 318–319, 88–112.

Heathwaite, A.L., Göttlich, K., Burmeister, E.G., Kaule, G. & Grospietsch, T. (1993) Mires: definitions and form. In: Heathwaite, A.L. & Göttlich, K. (eds.) *Mires: Process, Exploitation and Conservation*, Third Edition, John Wiley & Sons, Chichester, 1–64.

Hua, Q., Barbetti, M. & Rakowski, A.Z. (2013) Atmospheric radiocarbon for the period 1950–2010. *Radiocarbon*, 55(4), 2059–2072.

Joosten, H. & Clarke, D. (2002) *Wise Use of Mires and Peatlands: Background and Principles including a Framework for Decision-Making*. International Mire Conservation Group and International Peat Society, Saarijärvi, 304 pp.

Kassambara, A. (2017) *Practical Guide to Principal Component Methods in R*. STHDA, Marseille. Online at: www. sthda.com, accessed 25 Oct 2019.

Kelbe, B., Grundling, A. & Price, J. (2016) Modelling water table depth in a primary aquifer to identify potential wetland hydrogeomorphic settings on the northern Maputaland Coastal Plain, KwaZulu-Natal, South Africa. *Hydrogeology Journal*, 24(1), 249–265.

Maltby, E. & Barker, T. (eds.) (2009) *The Wetlands Handbook*. Blackwell Publishing, Chichester, 1058 pp.

Mitsch, W.J. & Gosselink, J.G. (2000) *Wetlands*. Third Edition, John Wiley & Sons, New York, 920 pp.

Mook, W. (2006) *Introduction to Isotope Hydrology: Stable and Radioactive Isotopes of Hydrogen, Oxygen and Carbon*. International Contributions to Hydrogeology 25, Taylor & Francis, London, 256 pp.

Mook, W. & van der Plicht, J. (1999) Reporting ^{14}C activities and concentrations. *Radiocarbon*, 43(3), 227–239.

Mucina, L. & Rutherford, M.C. (eds.) (2006) *The Vegetation of South Africa, Lesotho and*

Swaziland. Strelitzia 19, South African National Biodiversity Institute, Pretoria, 801 pp.

Naucke, W., Heathwaite, A.L., Eggelsmann, R. & Schuch, M. (1993) Mire chemistry. In: Heathwaite, A.L. & Göttlich, K. (eds.) *Mires: Process, Exploitation and Conservation*, Third Edition, John Wiley & Sons, Chichester, 486 pp.

Page, S.E., Wűst, R.A.J., Weiss, D., Rieley, J.O., Shotyk, W. & Limin, S.H. (2004) A record of Late Pleistocene and Holocene carbon accumulation and climate change from an equatorial peat bog (Kalimantan, Indonesia): implications for past, present and future carbon dynamics. *Journal of Quaternary Science*, 19(7), 625–635.

Porat, N. & Botha, G. (2008) The luminescence chronology of dune development on the Maputaland coastal plain, southeast Africa. *Quaternary Science Reviews*, 27(9–10), 1024–1046.

Reimer, P.J., Bard, E., Bayliss, A., Beck, J.W., Blackwell, P.G., Bronk Ramsey, C., Buck, C.E., Cheng, H., Edwards, R.L., Friedrich, M., Grootes, P.M., Guilderson, T.P., Haflidason, H., Hajdas, I., Hatté, C., Heaton, T.J., Hoffmann, D.L., Hogg, A.G., Hughen, K.A., Kaiser, K.F., Kromer, B., Manning, S.W., Niu, M., Reimer, R.W., Richards, D.A., Scott, E.M., Southon, J.R., Staff, R.A., Turney, C.S.M. & van der Plicht, J. (2013) IntCal13 and Marine13 radiocarbon age calibration curves 0–50,000 years calBP. *Radiocarbon*, 55(4), 1869–1887.

Schot, P.P. & van der Wal, J. (1992) Human impact on regional groundwater composition through intervention in natural flow patterns and changes in land use. *Journal of Hydrology*, 134(1–4), 297–313.

Stuyfzand, P.J. (1993) *Hydrochemistry and Hydrology of the Coastal Dune Area of the Western Netherlands*. PhD thesis, Free University of Amsterdam, 358 pp.

Thamm, A.G., Grundling, P. & Mazus, H. (1996) Holocene and recent peat growth rates on the Zululand coastal plain. *Journal of African Earth Sciences*, 23(1), 119–124.

Toth, J. (1963) A theoretical analysis of groundwater flow in small drainage basins. *Journal of Geophysical Research*, 68(16), 4795–4812.

van der Plicht, J., Wijma, S., Aerts, A.T., Pertuisot, M.H. & Meijer, H.A.J. (2000) Status report: The Groningen AMS facility. *Nuclear Instruments and Methods in Physics Research Section B: Beam Interactions with Materials and Atoms*, 172(1–4), 58–65.

van Loon, A.H., Schot, P.P., Griffioen, J., Bierkens, M.F.P., Batelaan, O. & Wassen, M.J. (2009) Throughflow as a determining factor for habitat contiguity in a near-natural fen. *Journal of Hydrology*, 379(1–2), 30–40.

von Post, L. (1922) Sveriges geologiska undersöknings torvinventering och några av dess hittills vunna resultat (The Geological Survey of Sweden peat inventory and some of its results). *Svenska Mosskulturföreningens Tidskrift*, 37, 1–27 (in Swedish).

Weitz, J. & Demlie, M. (2014) Conceptual modelling of groundwater-surface water interactions in the Lake Sibayi Catchment, Eastern South Africa. *Journal of African Earth Sciences*, 99, 613–624.

_____

Author for correspondence:
Professor Ab Grootjans, Nijenborgh 6, 9747 AG, Groningen, The Netherlands.   E-mail: a.p.grootjans@rug.nl

Appendix

Table A1. Overview of the observation tubes, their types, diameters, and depths and the sediment type Shaded cells indicate the tubes used during the 2015 sampling campaign.

No.	Campaign	Code	Depth (m)	Sediment type	Tube/instrument type
1	2015	S	0	-	River water
2	2015	VP 1	2.9	Sand	Piezometer
3	2015	VP 2	2.1	Sand	Piezometer
4	2015/2017	VP 3	3.9	Sand	Piezometer
5	2015	VNB 1p	1.3	Sand	Piezometer
6	2015	VNB1w	0.8	Peat	Dipwell
7	2015	VNB 2w	0.95	Peat	Dipwell
8	2015	VNB3p	2.2	Sand	Piezometer
9	2015	VNB3w	1	Peat	Dipwell
10	2015/2017	CW5	-	-	Manzengwenya Plantations well
11	2015	CW7	-	-	Community well
12	2015	CW8	-	-	Community well
13	2015/2017	CW6	-	-	Community well
14	2015	VNA1	2.1	Sand	Piezometer
15	2015	VNA 2w	0.8	Peat	Dipell
16	2015	VNA 2p	1.5	Sand	Piezometer
17	2015	VNA 3p1	2.4	Peat	Piezometer
18	2015	VNA 3w	1.25	Peat	Dipwell
19	2015	VNA 3p2	4	Sand	Piezometer
20	2015	VNA 4P2	1.6	Sand	Piezometer
21	2015	VNA4P1	1.12	Peat	Piezometer
22	2015	VNA 5	1.5	Sand	Piezometer
23	2015	VNC 1	1.9	Sand	Piezometer
24	2015	VNC 2	1.6	Sand	Piezometer
25	2015	VNC 3	1.65	Sand	Piezometer
26	2017	Pmu	1.8	Sand	Piezometer
27	2017	CW2	>10	Sand	Community well
28	2017	CW1	>10	Sand	Community well
29	2017	CW3a	0.2	Sand	Community well
30	2017	CW3b	>10	Sand	Community well
31	2017	PSF	0.2	Sand	Piezometer
32	2017	Pmag	1.5	Sand	Piezometer
33	2017	Pmat	1.5	Sand	Piezometer
34	2017	RGe	0	-	River water
35	2017	CW9	46	Sand	Community well
36	2017	Rain	Rain	-	Raingauge
37	2017	CW4	>10	Sand	Community well
38	2017	VN	3.5	Sand	Dipwell
39	2017	PKw	1	Sand	Dipwell
40	2017	Rsi	0	-	River water

Table A2: Ionic composition of the water samples collected from the Vasi peatland complex in 2015. All the macro ions are reported in mg L^{-1}.

No.	Code	pH	NO$_3$	Cl	SO$_4$	PO$_4$	HCO$_3$	Na	K	Ca	Mg	Fe	NH$_4$	SiO$_2$	TDS
1	S	6.39	0.00	67	2	0.00	43	32	3	9	7	0.74	0.05	10	162
2	VP1	5.80	0.14	19	15	0.02	47	9	5	9	4	7.44	2.31	2	109
3	VP2	4.01	1.31	33	171	0.00	5	33	3	33	9	11.40	6.07	13	289
4	VP3	4.98	1.99	137	151	0.00	12	88	10	39	15	0.47	0.93	11	455
5	VNB1P	5.84	1.29	84	120	1.34	65	64	4	27	20	1.65	0.12	5	386
6	VNB1W	5.95	0.38	194	209	0.05	56	130	22	26	33	1.37	1.90	3	670
7	VNB2W	5.41	3.81	321	190	0.47	54	185	5	22	37	1.00	26.57	3	819
8	VNB3P	5.15	0.87	354	407	0.00	43	225	4	37	62	3.51	44.53	4	1134
9	VNB3W	5.71	0.00	201	5	0.00	127	82	4	30	14	3.17	27.09	14	464
10	CW51	6.56	0.27	125	10	0.00	52	63	5	18	9	0.00	0.09	9	282
11	CW6	4.81	1.87	48	10	0.43	7	22	2	6	4	0.04	0.03	10	101
12	CW7	4.71	2.02	51	5	0.00	37	20	2	8	7	0.00	0.03	6	132
13	CW8	5.31	2.17	63	5	0.41	11	27	2	7	5	0.00	0.04	9	122
14	VNA1	5.60	0.32	113	34	0.06	26	49	5	16	14	4.53	3.14	7	257
15	VNA2W	5.70	1.09	140	136	0.00	40	96	6	21	19	7.78	1.57	3	458
16	VNA2P	5.94	0.18	50	89	0.00	71	31	5	30	15	3.02	1.45	6	291
17	VNA3P1	5.94	1.15	184	1	0.00	163	89	6	34	15	8.49	15.74	21	494
18	VNA3W	5.53	2.48	297	149	0.00	71	177	4	22	34	2.78	15.08	4	757
19	VNA3P2	6.20	0.66	126	1	0.00	245	55	6	58	10	14.17	18.18	33	501
20	VNA4P2	5.73	1.22	197	41	0.00	55	102	5	16	11	1.66	18.18	19	429
21	VNA5	5.54	1.26	180	143	0.00	43	109	5	26	18	3.11	15.28	7	525

Table A3. Ionic composition of the water samples collected from the Maputaland Coastal Plain in October 2017. All the macro ions are reported in mg L^{-1}.

No.	Code	pH	Cl	SO$_4$	PO$_4$	HCO$_3$	Na	K	Ca	Mg	Fe	NH$_4$	SiO$_2$	TDS
1	Pmu	7.68	684	1826	18.01	655	725	54	260	131	0.53	0.42	51	4029
2	CW2	8.26	441	52	1.86	386	268	10	89	28	<0.01	0.41	45	1085
3	CW1	8.23	90	2	1.99	298	29	6	65	15	<0.01	0.26	35	359
4	CW3a	6.94	25	26	1.6	30	29	11	6	5	0.28	0.21	24	118
5	CW3b	7.2	35	0	1.22	41	27	3	4	5	<0.01	0.25	44	97
6	PSF	7.22	201	36	0.22	61	133	5	10	18	0.59	1.47	26	441
7	Pmag	7.58	123	8	4.24	123	72	53	17	13	0.03	0.04	19	353
8	Pmat	6.58	79	4	0.48	29	51	6	10	6	0.52	0.00	27	171
9	RGe	6.27	79	7	0.31	9	48	8	5	5	0.14	0.18	18	156
10	CW9	6.23	131	3	0.85	9	62	5	3	8	<0.01	2.44	18	228
11	CW6Rain	6.92	12	4	0.09	20	9	1	7	2	<0.01	0.89	1	47
12	CW4	6.31	48	3	0.3	9	29	2	3	3	<0.01	0.23	20	92
13	CW5	5.21	97	7	0.62	5	43	2	4	7	<0.01	0.20	10	165
14	CW6	6.27	42	6	0.4	11	29	1	3	2	0.19	0.03	28	90
15	VP3	3.2	53	131	3.61	0	37	5	8	6	1.19	0.68	34	247
16	VN	7.01	26	48	0.16	34	29	3	7	10	<0.01	0.06	12	140
17	PKw	6.9	70	18	6.15	98	53	7	10	8	0.49	0.02	52	219
18	Rsi	7.39	56	3	0.34	47	37	4	7	6	1.67	0.04	26	137

Table A4. Water levels (cm below ground surface) measured in the groundwater tubes (P = piezometer, W = (perforated) dipwell) during the period February–July 2015. Depth refers to the bottom of the tube.

		VNA2			VNA3		VNA4		VNA5	VNB1		VNB2	VNB4	
	Type	P	P	P	P	P	P	P	P	P	W	W	P	W
	Rel. height (cm)	0	0	0	-1.6	-1.6	-1.8	-1.8	-0.8	0	0	-0.5	-0.5	-0.5
	Depth (cm)	150	57.4	81.1	400	240	158	112	150	124	87	95.5	217	105
DATE	21 Feb		24	23		14		23			17			27
	20 Mar	39	31	35	35	49	55	49	110	33	30	62	41	62
	01 Apr	47	39	40	36	45	59	51	115	35	35	71	44	70
	08 Apr	47	39	44	43	45	58	53	116	36	39	68	45	70
	20 Apr	47	43	45	44	47	65	53	119	41	37	67		
	05 May	52	34	50	43	51	64	57	125	41	41	66	55	74
	09 May	53	48	53	45	52	69	58	121	42	42	75	51	78
	23 May	53	46	52	51	54	70	56	dry	45	43	78	53	80
	10 Jun	60	53	57	57	67	75	75	130	51	51	75	58	82
	24 Jun	58	56	64	64	53	74	78	135	53	51	dry	61	84
	03 Jly	97	dry	92	67	93	101	dry	dry	56	56	dry	60	dry